

29. OXYGEN- AND HYDROGEN-ISOTOPE AND TRACE-ELEMENT INVESTIGATIONS ON ROCKS OF DSDP HOLE 395A, LEG 45

S. Hoernes, H. Friedrichsen, and H. H. Schock, Abt. Geochemie der Mineralogie Institut der Universität, Wilhelmstr. 53, 74 Tübingen, F. R. G.

ABSTRACT

The ^{18}O contents of 22 whole-rock samples and 36 separated minerals of oceanic crust material from DSDP Leg 45 and the D/H (deuterium/hydrogen) composition of 7 whole-rock samples and 2 serpentines were analyzed. The D/H content increases with depth, as does the ^{18}O content.

Isotope equilibrium temperatures of several basalts were obtained; the ^{18}O content decreases slightly with lower isotope temperatures. The role of ocean water during the formation of magmatic rocks is discussed.

Serpentinization temperatures 280°C and 380°C were calculated from serpentine-magnetite isotope fractionations.

Five whole-rock samples and separated phenocrysts of plagioclase, olivine, clinopyroxene, magnetite, and serpentine were analyzed for Na, Rb, Cs, Ca, Sr, Ba, La, Ce, Nd, Sm, Eu, Gd, Tb, Dy, Tm, Yb, Lu, Sc, Cr, Fe, Co, Ni, Zn, Th, Hf, Ta, U, Au, and Sb, using instrumental neutron activation analysis.

Uniform REE (rare-earth element) distributions, with enrichment factors between 11 and 15 relative to chondrites, a distinct light REE depletion $(\text{La}/\text{Sm})_{\text{norm.}} \approx 0.55$, but no Eu anomaly, have been observed in the basaltic samples.

One serpentinized peridotite shows very low REE concentrations, only 0.2 times the chondrite value.

Trace-element analyses of different phenocryst phases revealed elements for each mineral that are sensitive indicators for fractional crystallization of partial melting processes: Eu, Eu/Sm, and Sr for plagioclase, Ni and Co for olivine, and light REE/heavy REE, Cr, and Sc for clinopyroxene.

Titanomagnetite was the main Fe-Ti-oxide phase. Zn, Ni, and Co are enriched in titanomagnetite, but remarkable concentrations of Hf, Ta, and Th were also found. Titanomagnetite was found to be an important carrier for REE. Because divalent Eu is not incorporated into titanomagnetite, pronounced negative Eu-anomalies are developed during crystallization if oxygen fugacity permits high $\text{Eu}^{2+}/\text{Eu}^{3+}$ in the melt.

INTRODUCTION

Garlick and Epstein (1966), Taylor (1968, 1974), and Magaritz and Taylor (1976) have demonstrated that many shallow intrusive and extrusive magmatic rocks have exchanged oxygen isotopes with meteoric ground water. The amount of meteoric water (depleted in ^{18}O) which percolated through the magmatic bodies at high temperatures, lowering the initial ^{18}O -value of silicate minerals, has been calculated. In several cases, more than one-third of the oxygen in the silicates has exchanged with the fluid phase. Similarly, extensive isotopic exchange between ocean-crust basalts and seawater should be expected during emplacement of the basalts. Low-temperature reactions yielding smectite minerals have been demonstrated by Muehlen-

bachs and Clayton (1972) on dredged and drilled ocean-crust basalts. Isotopic exchange at these low temperatures results in smectites with high $\delta^{18}\text{O}$ -values ($\delta^{18}\text{O}$ up to + 25 ‰), and a reacting fluid phase depleted in ^{18}O . Significant formation of clay minerals could lower the $^{18}\text{O}/^{16}\text{O}$ ratio of seawater with time. Muehlenbachs and Clayton (1972) suggest, however, that the ^{18}O enrichment of the seawater caused by high-temperature interaction with basalt is essentially cancelled by the depletion of the $^{18}\text{O}/^{16}\text{O}$ ratio in the seawater by formation of clay minerals. Hence, one would not expect a long-term variation in the $^{18}\text{O}/^{16}\text{O}$ ratio of seawater with time.

Until now, only a small part of the oceanic crust has been investigated and, in particular, the crust has been drilled to only about one-tenth of its total thickness.

Few data exist on material balance calculations concerning exchange reactions between basalts and seawater.

The aim of this study was to determine (1) the temperature of the last equilibration between the various silicate phases of the basalts, and (2) the general nature of the distribution of oxygen and hydrogen isotopes among the silicate phases.

For this investigation, as many minerals as possible from the available samples (phenocrysts and minerals of the fine-grained groundmass) were separated and analyzed for their oxygen isotope composition.

In addition, five selected samples were analyzed for their minor- and trace-element contents, including eleven rare-earth elements determined by INAA (instrumental neutron activation analysis), to compare the exchange mechanisms for major (oxygen) and trace elements.

EXPERIMENTAL PROCEDURES

Thirty-six minerals in 12 rock samples from Leg 45, Hole 395A, were separated by standard techniques. The weight of the samples was between 10 and 20 grams. The mineral samples and also 20 powdered whole-rock samples were analyzed for their oxygen isotope composition, using the BrF_5 method (Clayton and Mayeda, 1963) for extraction of oxygen. The method described by Godfrey (1962) was used to extract hydrogen from 9 whole-rock samples.

Oxygen and hydrogen isotope compositions are reported using common δ -notation relative to SMOW (standard mean ocean water) (Tables 1 and 2). Routine reproducibility of δ -values is typically 0.1 ‰ for oxygen, and 1 to 2 ‰ for hydrogen.

RESULTS AND DISCUSSION

Whole Rocks

The average oxygen isotope composition of 20 basalts (whole-rock samples) is + 7.65 ‰. Compared with unaltered mantle differentiates, ^{18}O in these altered basalts is enriched by 2 ‰ (Taylor, 1968; Muehlenbachs and Clayton, 1972). All whole rock $^{18}\text{O}/^{16}\text{O}$ ratios of the basalts are distinctly higher than those of the separated phenocryst minerals (Figure 1), and indicate that the groundmass is not in isotopic equilibrium with the phenocrysts. The basalt groundmass in these rocks has interacted with sea water at low temperatures (less than 100°C). Large amounts of seawater must have percolated through the ocean crust to yield an enrichment of 2 ‰ in $\delta^{18}\text{O}$ in the groundmass.

The $\delta^{18}\text{O}$ whole-rock values of the basalts show a slight increase with depth, with a sharp inflection between 300 and 340 meters, followed by a slight increase in $\delta^{18}\text{O}$ below 340 meters (Figure 2).

Near 340 meters depth in Hole 395A, a stratigraphic change occurs from a thick series of phyrlic (mainly ol-plag-phyric) basalts in the upper part to mainly aphyric basalts in the lower part. A variation of the $\delta^{18}\text{O}$ whole-rock values with depth similar to that

TABLE 1
Oxygen Isotope Data Leg 45, Hole 395A

Sample (Interval in cm)	Piece	Rock Type/Minerals	$\delta^{18}\text{O}$	Min-Fractionations	T (°C)
4-1, 90-100	9	gabbro	+ 5.9	plag-mag 3.0 cpx-mag 0.8 plag-opx 1.3 plag-cpx 2.2	920
		opx	+ 5.0		
		cpx	+ 7.2		
		mag	+ 4.2 ± 0.3		
4-2, 56-61	3	serpent.peridotite	+ 2.0 ± 0.2	serp-mag 6.7	280
		whole rock	+ 2.7		
		serp	- 4.0		
5-1, 115-120	16 G	aphyrlic basalt	+ 7.2 ± 0.2		
9-2, 17-28	3	aphyrlic basalt	+ 6.6 ± 0.05		
11-1, 56-66	1	aphyrlic basalt	+ 7.6 ± 0.1		
13-1, 55-60	1	whole rock fresh	+ 7.4		
		altered	+ 7.4		
		serpent.peridotite	+ 5.8	opx-chrom 0.9 serp-mag 5.5	380
		opx	+ 4.8		
		cpx	+ 4.5		
serp	+ 4.9				
chromite	- 1.0				
14-1, 87-99	12	plag-ol phyrlic basalt	+ 5.9	plag-mag 1.8 plag-ol 1.0 ol-mag 0.8	1220
		plag	+ 4.9		
		ol	+ 4.1		
14-2, 125-134	9	plag-ol phyrlic basalt	+ 6.8 ± 0.5	plag-mag 2.9 plag-ol 1.0 ol-mag 1.9	930
		whole rock	+ 5.8		
		plag	+ 4.8		
		ol	+ 2.9		
15-4, 86-91	1k	plag-ol phyrlic basalt	+ 7.1		
17-1, 69-75	9	whole rock	+ 8.2 ± 0.1		
25-1, 36-43	5	plag-ol-cpx phyrlic basalt	+ 8	plag-ol 0.4	
		whole rock	+ 5.7		
		plag	+ 5.3		
26-2, 33-42	1f	basalt	+ 7.7 ± 0.5	plag-ol 1.0 plag-cpx 0.4	
		whole rock	+ 5.7		
		plag	+ 4.7		
		ol	+ 5.3		
33-1, 70-77	8	basalt	+ 6.2 ± 0.2	plag-ol 0.8	
		whole rock	+ 5.9		
		plag	+ 5.1		
46-1, 88-94	8	aphyrlic basalt	+ 7.0 ± 0.05		
52-1, 45-50	1	microcryst.basalt	+ 6.2 ± 0.5		
56-3, 50-57	M	whole rock	+ 8.3 ± 0.2		
61-2, 75-85	5	aphyrlic basalt	+ 7.0 ± 0.2	plag-mag 2.4 plag-ol 1.0 cpx-mag 2.1 ol-mag 1.4	1020
		whole rock	+ 6.0		
		plag	+ 5.0		
		ol	+ 5.7		
		cpx	+ 3.6		
61-3, 90-110	7	dolerite	+ 7.0 ± 0.1	plag-mag 2.6 plag-ol 0.7 cpx-mag 2.1 ol-mag 1.9	990
		whole rock	+ 5.9		
		plag	+ 5.2		
		ol	+ 5.4		
		cpx	+ 3.3		
63-2, 80-90	16	dolerite	+ 7.5 ± 0.15		
		whole rock	+ 5.9		
		plag	+ 5.7		
64-1, 137-142	1j	dolerite	+ 8.3	plag-mag 2.1 plag-ol 0.6 ol-mag 1.5	1100
		whole rock	+ 5.9		
		plag	+ 5.3		
		ol	+ 3.8		
66-3, 71-79		aphyrlic basalt	+ 9.1 ± 0.1		
11-2, 100-106	12j	whole rock	+ 6.9 ± 0.5		
19-1, 135-138	16	plag-phyric basalt	+ 7.3 ± 0.2		
		whole rock	+ 7.3 ± 0.2		

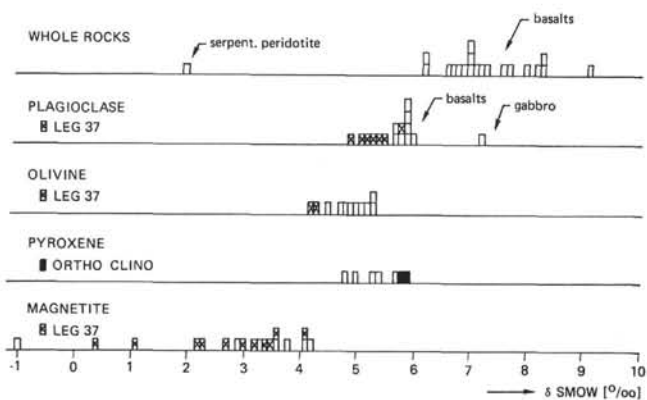
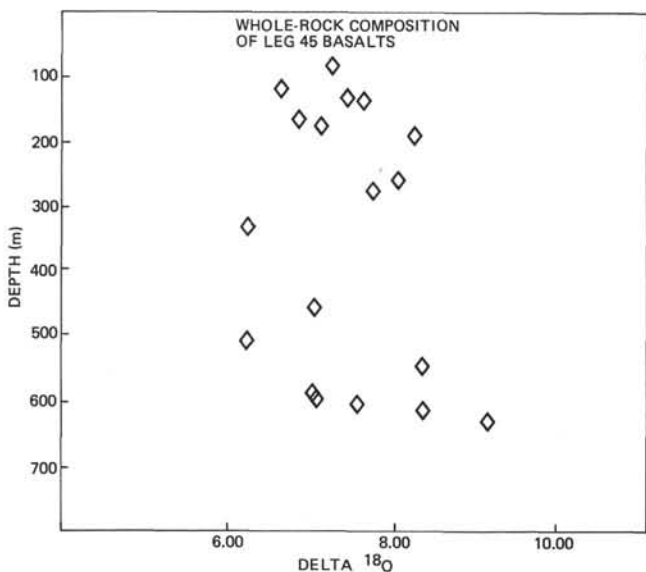
shown in Figure 2 was also found on Leg 37 (Hoernes and Friedrichsen, 1976).

Muehlenbachs and Clayton (1972) and Pineau et al. (1976) demonstrated that a relation exists between whole-rock $\delta^{18}\text{O}$ values and the water content of the basalts. A similar relationship can be calculated from our isotope data and the chemical analyses carried out by S. Lee in Munich (Figure 3). Since the only water-bearing mineral phases in these basalts are the smectite-minerals generated during alteration of the basalts,

TABLE 2
 $\delta D_{SMOW} - \text{Values } \text{‰}$

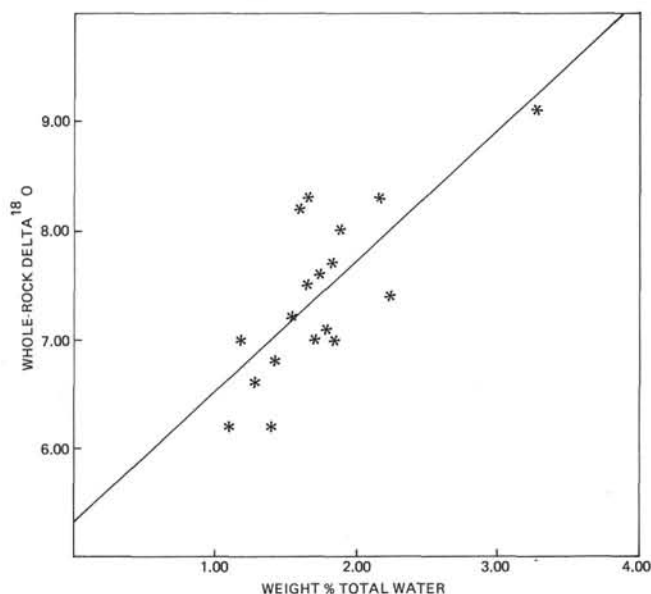
Sample (Interval in cm)	Piece	Sample	δD
4-2, 56-61	3	serpent.peridotite	- 60
5-1, 115-120	16G	aphyric basalt	- 118
11-1, 56-66	1	aphyric basalt	- 143
13-1, 55-60	1	serpent.peridotite	- 65
17-1, 69-75	9	plag-ol-cpx phyric basalt	- 135
33-1, 70-77	8	plag-ol phyric basalt	- 158
46-1, 88-94	8	aphyric basalt	- 123
61-2, 75-85	5	dolerite	- 86
64-1, 137-142	1j	dolerite	- 108

OXYGEN ISOTOPE COMPOSITION OF ROCKS AND MINERALS OF LEG 45 AND LEG 37


 Figure 1. Histograms of whole-rock and mineral $\delta^{18}\text{O}$ values.

 Figure 2. Whole-rock $\delta^{18}\text{O}$ variation with depth (Hole 395A), showing an inflection at 340 meters.

a relation between $\delta^{18}\text{O}$ of the rock and amount of clay minerals should be expected.

The δD values of seven whole-rock basalt samples and two serpentines were measured. The δD values of


 Figure 3. Correlation diagram of whole-rock $\delta^{18}\text{O}$ and weight % total H_2O . Coefficient of correlation $r = 0.76$.

the basalts vary between -85 and -158 ‰, and the two serpentines are around -60 ‰, despite their relatively large differences in $\delta^{18}\text{O}$. In Figure 4, δD is plotted against the depth of the recovered core, and a rough correlation between these parameters is apparent. The δD -value of the pore water is not known, but since the oxygen isotope variations in the altered rocks indicate that large amounts of seawater interacted with the basalts, a large amount of hydrogen must have been available during the formation of clay minerals. Deuterium enrichment in the pore fluids caused by preferred incorporation of protium in the solid phase is negligible, because the hydrous minerals represent only a tiny portion of the total hydrogen in the system. The variation in the δD content of the rocks is most likely a result of the formation of the clay minerals at different temperatures.

High-temperature fractionation of D and H between hydroxyl-bearing solids and water have been determined by Suzuoki and Epstein (1976). They found that a decrease in the equilibration temperature was accompanied by an increase in the hydrogen isotope fractionation between the solid phases and the H_2O , with the solid phase always depleted in D with respect to H_2O . The extrapolation of their data to lower temperatures is compatible with the large D/H fractionation between clay minerals and sea water implied in Figure 4.

Mineral Data

The minerals separated from Hole 395A rocks show a relatively small spread in $\delta^{18}\text{O}$ (Figure 1). Plagioclase in the basalt varies in $\delta^{18}\text{O}$ from $+5.7$ to $+6.0$ ‰, whereas plagioclase from a gabbro has a distinctly higher $\delta^{18}\text{O}$ value of $+7.2$ ‰. The $\delta^{18}\text{O}$ -values of the pyroxenes fall in a range of $+4.8$ to $+5.9$ ‰, the higher values for orthopyroxenes. Olivines have $\delta^{18}\text{O}$ values of $+4.7$ to $+5.3$ ‰. The magnetites from basalts

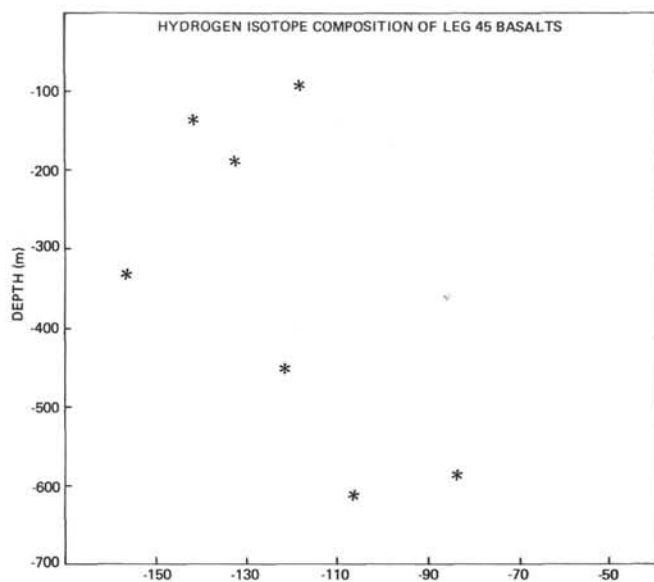


Figure 4. Hydrogen isotope variation of some basalt whole-rock samples, showing a slight increase of the D/H ratios with depth.

show a relatively large spread in $\delta^{18}\text{O}$, from 2.9 to 4.2 ‰.

Plagioclase and olivine from Leg 45 have significantly higher $\delta^{18}\text{O}$ values than rocks from Leg 37. This seems to indicate differences in the oxygen isotope composition of the magmas, resulting from exchange with the oxygen-rich seawater. Secondary magnetites, which formed as products of serpentinization of peridotites, have $\delta^{18}\text{O}$ values of -2 to -4 ‰, and coexisting serpentines have $\delta^{18}\text{O}$ values of $+2.7$ and $+4.0$ ‰.

Geothermometry

The fractionation of oxygen isotopes between co-genetic minerals can be used to estimate the temperature of last equilibration of oxygen isotopes in the system. In the case of magmatic rocks this is, or is close to, the crystallization temperature. A good indication for isotope equilibrium in rocks is concordant isotope temperatures for more than one mineral pair.

In Figure 5, $\Delta^{18}\text{O}$ (plagioclase/magnetite) is plotted versus $\Delta^{18}\text{O}$ (olivine/magnetite). With few exceptions the values for most rocks plot on the "concordancy curve." Temperature calibration points on this curve were calculated from the plagioclase-water curve of O'Neil and Taylor (1967) for a plagioclase of An_{60} and the magnetite-water curve of Bertenrath et al. (1972).

In Figure 6, the plagioclase-magnetite isotope fractionation is plotted against $\delta^{18}\text{O}$ -magnetite. In Figure 7, the plagioclase-olivine isotope fractionation is plotted against $\delta^{18}\text{O}$ -olivine. A regression curve in both diagrams indicates that the δ -values of both magnetite and olivine change with the Δ plagioclase-magnetite and Δ plagioclase-olivine isotope fractionations. But it appears that the change in the δ -values of the above phases is higher than the change of the fractionation values. If we calculate the whole-rock isotopic composition

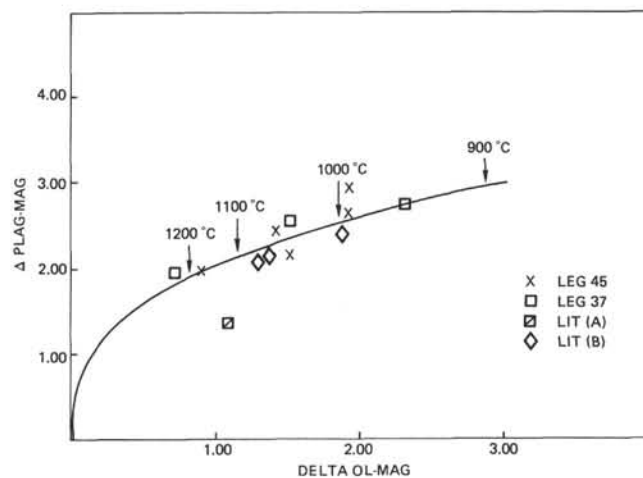


Figure 5. "Concordancy diagram" of Δ plagioclase-magnetite against Δ olivine-magnetite. Lit. A: Muehlenbachs and Clayton (1972). Lit. B: Anderson et al. (1971).

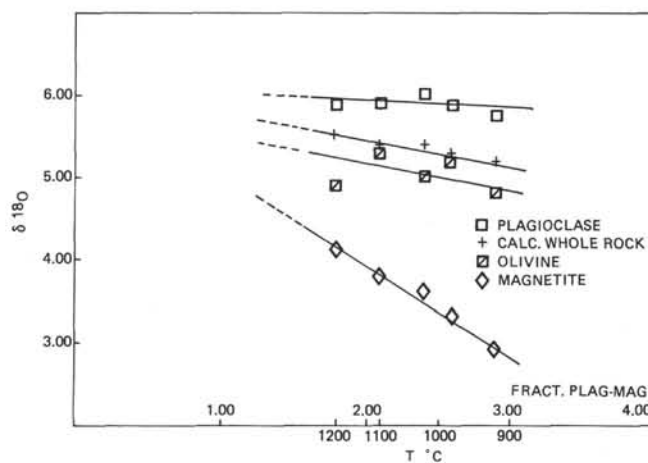


Figure 6. Plot of $\delta^{18}\text{O}$ plagioclase, magnetite, olivine, and a calculated whole-rock isotopic composition versus the plagioclase-magnetite fractionation. The whole-rock composition is calculated from the mineral data presented in Table 1 and an estimated modal composition.

tion from the composition of these phases, it seems that there is a slight $^{18}\text{O}/^{16}\text{O}$ decrease of the whole rocks with the higher Δ values of both mineral pairs. These data are summarized in Figure 6. If the decrease of the whole-rock isotopic composition is caused by an addition of seawater—which to us is the only light-oxygen-isotope source for these rocks—then the decrease of the crystallization temperature (or increase of both mineral pair fractionations) is caused by seawater.

Therefore, seawater has interacted with the silicates at magmatic temperatures, and the increase of the water pressure has decreased the crystallization temperature.

Metamorphic reactions in either basalts or peridotites yield rocks of low ^{18}O -composition. The Hole 395 serpentinized peridotites are reduced in their oxygen isotope content by 2 to 4 ‰, which can only be accom-

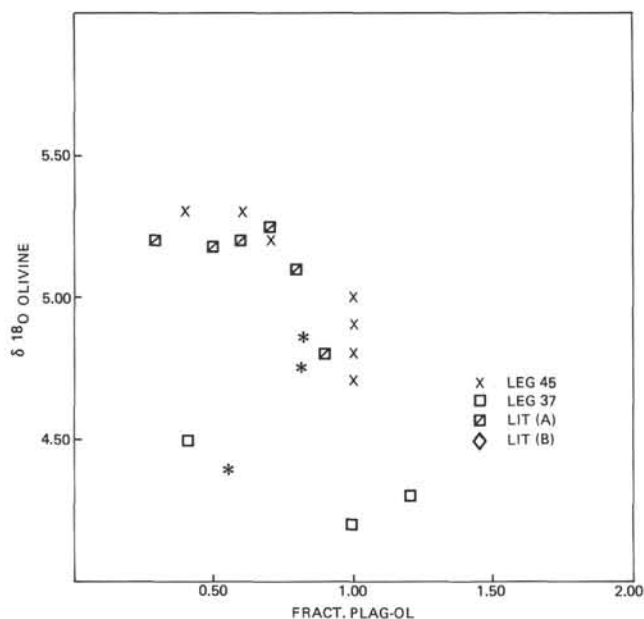


Figure 7. Plot of $\delta^{18}\text{O}$ olivine versus the plagioclase-olivine fractionation. Lit. A, B, see Figure 5.

plished by a 10 to 30 per cent oxygen contribution from the seawater. Peridotites which reacted with higher amounts of seawater yielded lower serpentinization temperatures (derived from serpentine-magnetite fractionations) of 280°C ; those peridotites which were partly serpentinized yielded a serpentinization temperature of 380°C . For calculating these temperatures, the isotope thermometer of Wenner and Taylor (1973) has been applied.

Further detailed studies are necessary to calculate whether a low-temperature interaction of the basalts, with a decrease of the $^{18}\text{O}/^{16}\text{O}$ -ratio of the seawater, or a high-temperature reaction, with an increase of the $^{18}\text{O}/^{16}\text{O}$ -ratio of the seawater, is dominant.

Trace-Element Investigations

Whole-rock samples of two plagioclase-olivine-phyric basalts (Sections 395A-14-2 and 395A-25-1), two samples of the plagioclase-olivine-phyric dolerite (Sections 395A-61-3 and 395A-63-2) and one highly serpentinized peridotite (Section 395A-4-2) were selected for trace-element analyses. Concentrations were determined after a two-day irradiation of samples and single-element standards with $7 \cdot 10^{13}$ n/cm²s, followed by instrumental analysis according to methods published elsewhere in greater detail (Schock, 1973, 1977a). The results are presented in Table 3, together with those of separated minerals.

If rare earth element (REE) concentrations are normalized to chondritic abundances, remarkably uniform distribution patterns are obtained for the basaltic samples (Figure 8). All curves show a distinct light REE depletion [$(\text{La}/\text{Sm})_{\text{norm.}} \approx 0.55$]. The distribution of elements heavier than Nd is almost pure chondritic, with an over-all enrichment factor that varies only between 11 and 15. (The small, but significant deviation of the Yb values from the smooth curve is not under-

stood at present.) These patterns resemble in all details those observed in samples of Leg 37, Site 335 (Blanchard et al., 1976; O'Nions and Pankhurst, 1976).

The REE compositions of the two doleritic samples and of one basalt sample (Section 395A-25-1) are identical, within the limits of error. This would support the presumption that the doleritic unit is an intrusive equivalent of some basalts sampled in higher parts of the hole (Chapter 7, this volume). The significantly higher REE contents of the second basaltic sample (Section 395A-14-2) from the uppermost phyrlic unit indicates a higher degree of fractionation, which can also be seen in elevated contents of some large, high-valency cations like Hf and Th, and in the relatively low contents of Cr and Ni. On the other hand, nearly identical concentrations of Sc (about 34 ppm) are rather surprising.

A Eu anomaly was observed in none of the samples; hence, in all differentiation processes that took place before eruption of the melts, only very limited amounts of plagioclase could have been involved.

From the ultramafic rocks only an almost completely serpentinized peridotite was analyzed. Its REE contents were very low, about two orders of magnitude below basaltic samples, or one-fifth of normal chondritic concentrations; for that reason, only five elements could be determined. The REE distribution pattern (Figure 8) seems not to be chondritic or light-REE depleted; on the contrary, a significant enrichment of La over Sm was found. Whether this observation reflects the REE distribution of the original peridotite or whether this is only a secondary effect caused by the serpentinization, cannot be answered definitely. The effect of serpentinization on REE distribution is still controversial, but light REE depletion is favored (c.f. Menzies, 1976). Of course, this conflicts with our observation that there is marked enrichment of La in the serpentine separate (Table 3). Also, Sc clearly behaves in another manner than the REE; its content in this peridotitic sample is only 5 times below that of basaltic samples.

Among transition elements, Fe, Co, and Zn concentrations are comparable to those in the basalts, whereas the Ni content (1600 ppm) is more than 10 times and Cr content (1500 ppm) is about 5 times higher than in basalts. Additionally, we found about 30 ppb of Au and 150 ppb of Sb in the peridotites.

Plagioclase

Plagioclases from four different rock samples were analyzed (Table 3). Three of them show nearly identical anorthite contents (An_{76-78}), whereas one plagioclase separate from one of the doleritic samples has an An-content of only 67. Total iron (as FeO) varies between 0.5 per cent and 0.7 per cent.

If we look at the distribution of REE as a function of their ionic radii, relative concentrations show a monotonous increase from Lu to La, as trivalent REE ions fit successively better into the Ca sites of the plagioclase structure. This trend can also be seen in Figure 9, where REE contents are normalized to whole-rock

TABLE 3
Elemental Concentrations (ppm) in Whole-Rock and Mineral Samples From Leg 45, Hole 395A

Element	Sample 14-2, 125-134 cm, Piece 9				Sample 25-1, 36-43 cm, Piece 5		Sample 4-2, 56-61 cm, Piece 3			
	Whole Rock 42.5 mg	Plagioclase 87.2 mg	Olivine 7.41 mg	Magnetite 40.4 mg	Whole-Rock 37.64 mg	Plagioclase 83.76 mg	Whole-Rock 79.2 mg	Serpentine 48.7 mg		
Na	21100 ±300	17600	230	2200	19130	18000	500	215		
Rb	< 6	0.8	< 9	55	< 7	< 0.3	< 7	< 5		
Cs	< 0.25	0.05	< 0.3	0.3	< 0.27	0.04	< 0.22	< 0.02		
Ca ^a	64500	112000	20000	10300	84500	109000	380	1250		
Sr ^a	160	200	< 50	< 20	145	162	< 5	< 5		
Ba	< 55	< 2	< 40	< 65	< 60	< 2	< 35	< 35		
La	3.0 ±0.25	0.24	0.003	5.5	2.1	0.18	0.10	0.90		
Ce	8.8 ±0.6	0.80	0.04	13.1	7.5	0.52	0.16	0.6		
Nd	9.2 ±1.8	0.62	< 0.25	14.6	9.9	0.33	< 0.38	< 0.8		
Sm	3.18 ±0.04	0.152	0.003	4.39	2.61	0.103	0.021	0.027		
Eu	1.19 ±0.02	0.281	0.04	1.01	1.01	0.226	0.015	0.03		
Gd	4.2 ±0.8	b	< 0.15	4.6	3.2	b	< 0.4	< 0.9		
Tb	0.70 ±0.04	0.022	< 0.004	0.80	0.57	0.018	< 0.008	< 0.02		
Dy	5.3 ±0.5	0.17	< 0.004	5.2	3.8	0.16	< 0.10	< 0.17		
Tm	0.52 ±0.04	0.013	0.003	0.59	0.35	0.007	—	< 0.03		
Yb	2.73 ±0.07	0.089	0.07	2.7	2.30	0.052	0.04	0.10		
Lu	0.54 ±0.05	0.014	< 0.015	0.50	0.42	0.011	< 0.025	< 0.025		
Sc	34.1 ±0.2	0.56	6.46	17.7	33.4	0.67	6.90	18.1		
Ti ^a	11500	1550	—	144000	9530	2950	2400	3000		
Cr	228 ±4	10.4	264	29	315	8.0	1480	2525		
Fe	65000 ±600	4160	94200	497000	61700	3950	58100	19700		
Co	77.7 ±0.5	1.48	139.1	165	92.7	1.11	90.3	41.9		
Ni ^a	100	130	1410	320	180	100	1550	1500		
Zn ^a	88	60	110	880	165	45	65	88		
Th	0.20 ±0.25	0.004	0.21	0.67	< 0.16	< 0.005	< 0.12	< 0.12		
Hf	2.04 ±0.04	0.063	< 0.015	5.6	1.71	0.037	< 0.03	< 0.07		
Ta	0.31 ±0.02	0.0045	< 0.002	0.83	0.45	0.0020	2.35	< 0.01		
U	< 0.12	0.012	< 0.03	< 0.18	0.07	0.001	0.43	0.82		
Au	—	—	—	0.15	0.050	—	0.027	—		
Sb	< 0.03	0.018	—	0.17	0.03	0.012	0.14	0.28		
	Sample 61-3, 90-110 cm, Piece 7					Sample 63-2, 80-90 cm, Piece 16				
Element	Whole-Rock 38.1 mg	Plagioclase 42.9 mg	Clino-pyroxene 4.95 mg	Olivine 11.0 mg	Magnetite 29.0 mg	Whole-Rock 40.5 mg	Plagioclase 113.1 mg	Clino-pyroxene 6.28 mg	Olivine 9.70 mg	Magnetite 25.4 mg
Na	18400	15100	4600	—	2400	19200	14900	5900	3200	1640
Rb	< 6	0.8	< 15	< 5	< 16	< 6	1.1	< 16	< 6	62
Cs	< 0.26	0.11	< 0.8	< 0.13	< 0.45	< 0.26	0.12	< 0.9	< 0.9	1.4
Ca ^a	80000	112500	137000	4200	10100	83000	97000	140000	18000	10000
Sr ^a	120	156	< 230	—	< 20	130	185	< 190	—	< 20
Ba	< 45	1.6	< 170	< 25	< 90	< 50	< 2	< 190	< 30	< 150
La	2.2	0.14	0.36	0.02	3.3	2.4	0.39	0.6	0.08	4.2
Ce	7.5	0.47	2	< 0.1	7.8	8.3	1.1	1	< 0.2	10
Nd	8.8	0.16	< 3	0.2	17	7.2	0.89	2	< 0.15	12
Sm	2.63	0.077	1.5	0.01	2.83	2.73	0.231	1.40	0.02	3.3
Eu	1.02	0.215	0.56	0.009	0.64	1.03	0.378	0.57	0.03	0.62
Gd	3.1	b	3.7	< 0.2	3.4	3.4	b	< 2	< 0.4	5.4
Tb	0.56	0.018	0.47	0.002	0.68	0.59	0.047	0.46	< 0.008	0.58
Dy	3.8	0.10	2.6	< 0.2	3.7	4.2	0.20	3.7	< 0.05	4.8
Tm	0.43	0.004	0.68	0.010	0.49	0.43	0.021	0.59	< 0.01	0.59
Yb	2.34	0.053	1.88	0.07	2.1	2.3	0.13	1.8	0.039	2.4
Lu	0.44	0.0063	0.72	< 0.012	0.40	0.45	0.019	0.70	< 0.013	0.46
Sc	34.3	0.675	104	6.24	19.9	34.8	0.48	95.8	5.40	23.3
Ti ^a	9800	1450	—	—	141000	12000	800	—	—	152000
Cr	334	37	4530	349	13.3	360	3.4	4020	290	30
Fe	63200	4410	48100	99600	478000	62700	5900	37000	84100	459000
Co	92.8	0.71	38.1	153	208	77.2	3.25	36.5	128	135
Ni ^a	130	160	< 600	1530	780	180	130	< 650	1300	470
Zn ^a	105	85	—	75	900	110	140	—	80	900
Th	< 0.14	< 0.005	< 0.5	< 0.07	< 0.24	< 0.15	0.016	< 0.5	< 0.08	0.55
Hf	1.65	0.020	0.7	< 0.02	5.4	1.77	0.11	0.4	< 0.03	7.5
Ta	0.70	0.0030	< 0.02	< 0.003	0.84	0.46	0.004	< 0.02	< 0.004	1.08
U	< 0.10	< 0.015	< 0.25	< 0.05	0.2	< 0.10	< 0.01	< 0.2	0.02	< 0.2
Au	0.013	—	—	—	—	—	—	—	0.01	0.019
Sb	< 0.03	0.25	—	—	—	< 0.03	0.008	—	—	0.10

^aIn most cases (whole-rock, plagioclase, magnetite), determination by atomic absorption spectrometry.

^bGd determination in feldspars using ¹⁵²Gd(n,γ) ¹⁵³Gd is strongly impeded, because ¹⁵²Gd is produced from Eu during neutron irradiation according to ¹⁵¹Eu(n,γ) ¹⁵²Eu(9.5h) → ¹⁵²Gd.

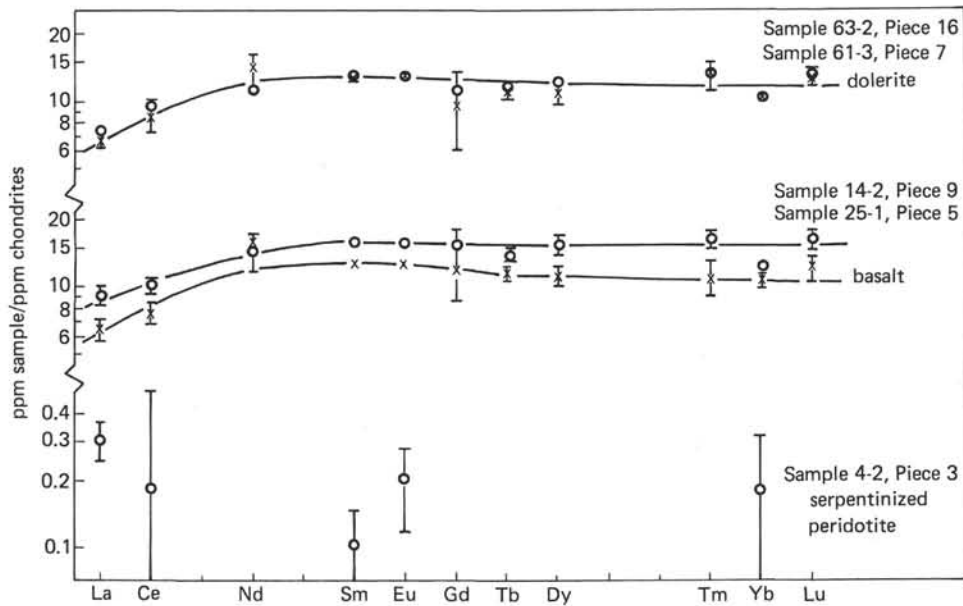


Figure 8. Concentration of the REE in Leg 45 samples normalized to chondritic abundances (data from Nakamura, 1974 and 0.050 ppm for Tb).

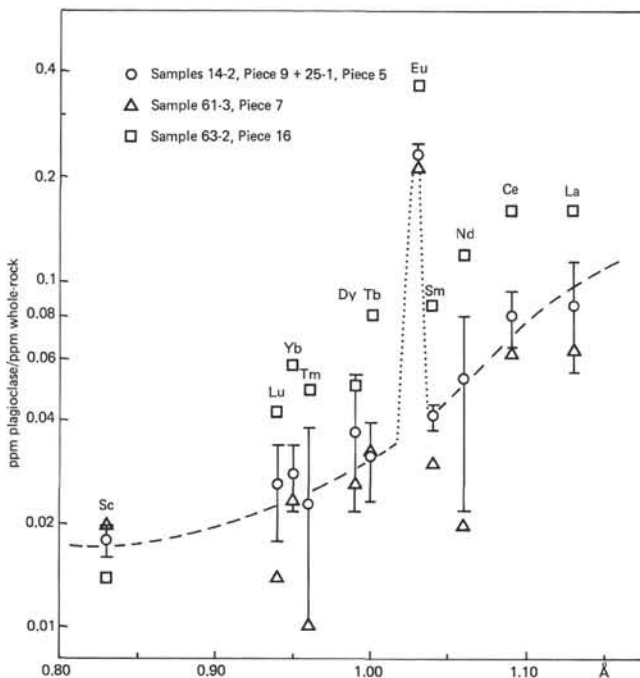


Figure 9. REE concentrations of plagioclases relative to whole-rock composition versus ionic radius. Ionic radii from Whittaker and Muntus (1970). Error bars include standard deviation (σ_2) of each sample counting rate.

compositions and give a type of partition coefficient. These values are of the same order of magnitude as those reported from experimental (e.g., Drake and Weill, 1975) or analytical (e.g., Higuchi and Nagasawa, 1969) investigations on systems of basaltic composition.

In the case of the two basalt samples (Sections 395A-14-2 and 25-1), the difference in REE content is

also reflected by a similar difference in the plagioclase separates. By contrast, the REE concentrations of the plagioclases from the dolerite differ by a factor of 2.5, although there is no difference between the whole-rock contents. Of course, it must be mentioned that the plagioclase with the higher REE content is less calcic than all others (An_{67} compared with An_{76-78}). Nevertheless, such a striking difference in REE concentrations is not easy to understand. In principle, there exist two possible origins. Assuming constant partition coefficients, the melt from which these plagioclases crystallized was either strongly enriched in REE or partition coefficients were 2 to 3 times higher, for instance because of a lower crystallization temperature. But the temperature dependence of REE partition coefficients is not strong (Drake and Weill, 1975) and, additionally, there is no corroborative indication from oxygen isotope data for differences in crystallization temperature. Moreover, the difference in Eu concentrations is only a factor of 1.7, apparently caused by a lower Eu^{2+} concentration in the melt. In addition, elements like Co, Zn, Hf, and Th are also enriched in the plagioclase sample with the higher REE contents, whereas Sc and Cr are markedly depleted. This all points to crystallization of this plagioclase from a melt differentiated to a higher degree. Finally, magnetites separated from the same dolerite sample show elevated REE contents too.¹

Olivine

Olivines from three different samples were analyzed (Table 3). Because of scarcity of very pure material and of tiny concentrations of many elements, only

¹ Editor's note: Rhodes et al. (this volume) support this argument by suggesting mixing between a 'primitive' magma with high-An plagioclases and a fractionated magma with lower-An plagioclases.

about 12 elements containing 4 or 5 REE could be determined by instrumental analysis.

From Fe analyses, we calculate a compositional range from Fa_{10} to Fa_{15} . High contents of Ni (1300 to 1500 ppm) and Co (130-150 ppm) and moderate concentrations of Cr (250 to 350 ppm) and Zn (80-110 ppm) were found. If these data are divided by the corresponding whole-rock concentrations, the resulting partition coefficients decrease in the order $Ni > Co > Fe > Cr > Zn$. That is in agreement with analytical data from Henderson and Dale (1970) and Gunn (1971), and reflects the differences in octahedral site preference energy of these transition elements in the olivine structure.

REE concentrations in olivine are very low, and many are below the detection limit for instrumental neutron activation analysis. In all cases, the data are comparable to those determined by Higuchi and Nagasawa (1969) and Mysen (1976). A slight preference for heavy REE (because of their smaller size) should be expected in olivines (Higuchi and Nagasawa, 1969). This is underscored by the much better incorporation of the still smaller Sc ion. Nevertheless, even this ion is too large for octahedral sites of the olivine structure. Therefore, its partition coefficient in olivine is only about 0.2, and during crystallization of olivine, Sc is enriched in the melt.

Clinopyroxene

Two samples of clinopyroxene (about 5 mg each) separated from the dolerite have been analyzed (Table 3). Ca contents are about 14 per cent and Fe contents are 4.8 per cent and 3.7 per cent, respectively. REE concentrations are relatively high and of the same order of magnitude as in the whole-rock samples. This is because of the presence of sites in the clinopyroxene structure which are large enough to accept trivalent REE in appreciable amounts. Not all REE were incorporated to the same extent, however. If normalized REE concentrations are plotted against ionic radius (Figure 10), a strong increase from La to the heavier REE is evident. This trend of the curve and the absolute values agree with experimental results (Masuda and Kushiro, 1970; Grutzeck et al., 1968; Schock, 1977b), if one disregards the two deviating points for Tm and Lu (Figure 10). In nearly all REE partition coefficient investigations, a broad maximum near the ionic radius of Dy has been found, indicating of optimal ionic size for incorporation into the Ca position of the clinopyroxene structure.

No Eu anomaly is observed in the clinopyroxenes, and normalized concentrations of Sm and Eu are equal, within the limits of error. This may be attributed to incorporation of both Eu^{3+} and Eu^{2+} into the structure to a similar degree. Experimental studies (Sun et al., 1974; Weill et al., 1974) indicate that, although the partition coefficient for trivalent Eu in clinopyroxene exceeds that for divalent Eu, the difference in partition coefficients is not as extreme as in the case of plagioclase.

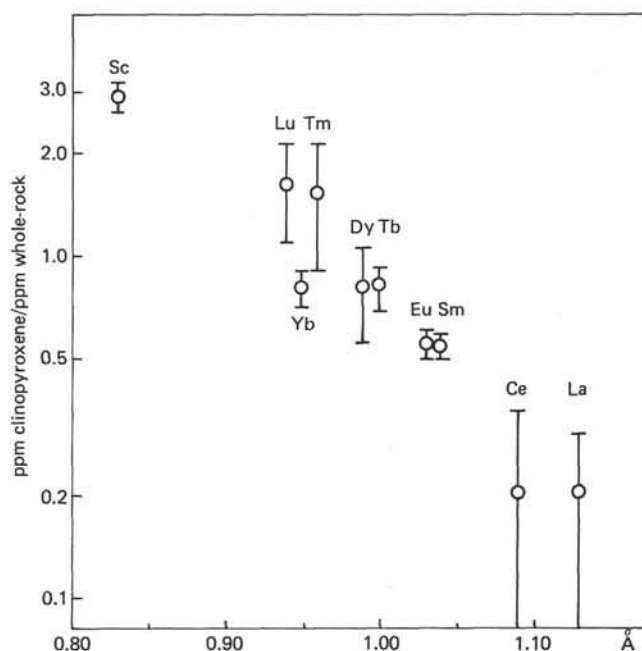


Figure 10. REE concentrations of two clinopyroxenes, Samples 61-3, Piece 7, and 63-2, Piece 16, relative to whole-rock composition versus ionic radius. Ionic radii from Whittaker and Muntus (1970).

We found, among other trace elements, very high contents of Cr and Sc in clinopyroxenes. Normalized to whole-rock compositions, the partition coefficient of Cr is >10 and Sc is about 3. Because of their smaller ionic radii, we conclude that these elements are preferentially incorporated into the smaller six-coordinate Mg-sites of the structure, Sc as a trivalent and Cr as a divalent ion. Co, another divalent ion, is accepted to a distinctly lesser degree, with a partition coefficient of about 0.4. In spite of its high charge, Hf^{4+} seems to fit into the Mg-site, and therefore it is incorporated in appreciable amounts.

Magnetite

Three magnetic separates were analyzed (Table 3). They all consist of titanomagnetite; only traces of ilmenite could be detected by X-ray methods. TiO_2 varies between 24 and 25 per cent, the same order of magnitude as determined for titanomagnetites separated from Leg 34 samples (Mazzullo and Bence, 1976).

Surprisingly, we found many trace elements in magnetite. Relatively high amounts of Ca (about 1%) and Na (about 0.2%) were detected. If elemental concentrations are normalized to whole-rock composition, Zn is the element with the highest enrichment factor (8 to 10), followed by Ni (3 to 5) and Co (about 2), whereas Cr (about 0.1) is extremely depleted. This relates to an appreciable depletion of Cr already present in the fractionated liquids from which these magnetites crystallized, and demonstrates that whole-rock compositions are not well suited for normalization, at least in the case of magnetite. Nevertheless, the high concen-

tration of large high-valency cations like Hf, Ta, and Th is remarkable.

Most surprising are the high concentrations of REE. From structural considerations and comparisons of ionic radii, a marked depletion of REE in titanomagnetites should be expected. But, on the contrary, equivalent or even higher contents than the whole-rock samples were measured. If whole-rock normalized REE concentrations are plotted against ionic radius (Figure 11), only a very flat pattern can be observed, with an increasing tendency towards higher ionic radius.

All samples of magnetite show a strong negative Eu-anomaly (Figure 11). This is caused by an effect similar to that in the plagioclases, but in the magnetite structure, Eu^{3+} is preferred to Eu^{2+} . If Eu^{3+} concentration in the melt is substantially lower than the normalized concentrations of other trivalent REE, which is true for all deep-sea basalts, this must lead to negative Eu-anomalies in magnetite as a reflection of a positive Eu-anomaly in the plagioclases.

ACKNOWLEDGMENTS

This work was supported by grants of the Deutsche Forschungsgemeinschaft DFG Fr 357/7, 9, 11. Neutron activation of the samples was supported by resources of the Gesellschaft für Kernforschung mbH Karlsruhe.

REFERENCES

- Anderson, A. T., Jr., Clayton, R. N., and Mayeda, T. K., 1971. Oxygen isotope thermometry of mafic igneous rocks, *J. Geology*, v. 79, p. 715-729.
- Bertenrath, R., Friedrichsen, H., and Hellner, E., 1973. Die Fraktionierung des Sauerstoffisotops ^{16}O und ^{18}O im System Magnetit/Wasser, *Fortschr. Miner.*, v. 50, p. 32-33.
- Blanchard, D. P., Rhodes, J. M., Dungan, M. A., Rodgers, K. V., Donaldson, C. H., Brannon, J. E., Jacobs, J. E., and Gibson, E. K., 1976. The chemistry and petrology of basalts from Leg 37 of the Deep Sea Drilling Project, *J. Geophys. Res.*, v. 81, p. 4231-4246.
- Clayton, R. N. and Mayeda, R. K., 1963. The use of bromine pentafluoride in the extraction of oxygen from oxides and silicates for isotopic analysis, *Geochim. Cosmochim. Acta*, v. 27, p. 43-52.
- Drake, M. J. and Weill, D. F., 1975. Partition of Sr, Ba, Ca, Y, Eu^{2+} , Eu^{3+} , and other REE between plagioclase feldspar and magmatic liquid: an experimental study, *Geochim. Cosmochim. Acta*, v. 39, p. 689-712.
- Garlick, G. D. and Epstein, S., 1966. The isotopic composition of oxygen and carbon in hydrothermal minerals at Butte, Montana, *Econ. Geol.*, v. 61, p. 1325-1335.
- Godfrey, J. D., 1962. The deuterium content of hydrous minerals from the East-Central Sierra Nevada and Yosemite National Park, *Geochim. Cosmochim. Acta*, v. 26, p. 1215-1245.
- Grutzeck, M., Kridelbaugh, S., and Weill, D., 1974. The distribution of Sr and REE between diopside and silicate liquid, *Geophys. Res. Lett.*, v. 1, p. 273-275.
- Gunn, B. M., 1971. Trace element partition during olivine fractionation of Hawaiian basalts, *Chem. Geol.*, v. 8, p. 1-13.
- Henderson, P. and Dale, I. M., 1970. The partitioning of selected transition element ions between olivine and groundmass of oceanic basalts, *Chem. Geol.*, v. 5, p. 267-274.

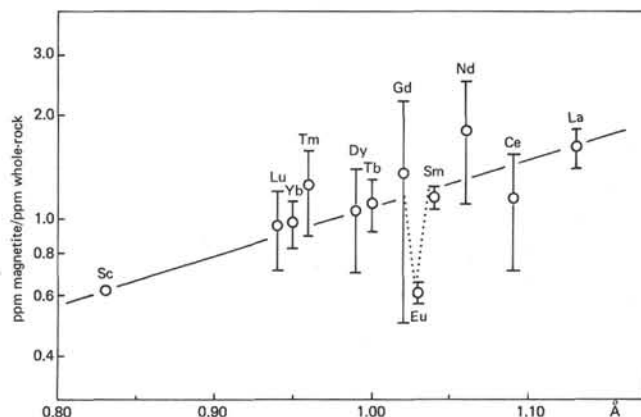


Figure 11. REE concentrations of two magnetites, Sections 61-3 and 63-2, relative to whole-rock composition versus ionic radius.

- Higuchi, H. and Nagasawa, H., 1969. Partition of trace elements between rock-forming minerals and host volcanic rocks, *Earth Planet. Sci. Lett.*, v. 7, p. 281-287.
- Hoernes, S. and Friedrichsen, H., 1976. Oxygen isotope investigations of rocks of Leg 37. In Aumento, F., Melson, W. G., et al., *Initial reports of the Deep Sea Drilling Project*, v. 37: Washington (U. S. Government Printing Office), p. 603-606.
- Magaritz, M. and Taylor, Jr., H. P., 1976. $^{18}\text{O}/^{15}\text{O}$ and D/H studies along a 500 km traverse across the Coast Range batholith and its country rocks, central British Columbia, *Canadian J. Earth Sci.*, v. 13, p. 1514-1536.
- Masuda, A. and Kushiro, I., 1970. Experimental determination of partition coefficients of ten rare earth elements and barium between clinopyroxene and liquid in the synthetic silicate system at 20 kbar pressure, *Contrib. Mineral. Petrol.*, v. 26, p. 42-49.
- Mazzullo, L. J. and Bence, A. E., 1976. Abyssal Tholeiites from DSDP Leg 34: The Nazca plate, *J. Geophys. Res.*, v. 81, p. 4327-4351.
- Menzies, M., 1976. Rare earth geochemistry of fused ophiolitic and alpine lherzolites - I. Othris, Lanzo and Troodos, *Geochim. Cosmochim. Acta*, v. 40, p. 645-656.
- Muehlenbachs, K. and Clayton, R. N., 1972. Oxygen isotope studies of fresh and weathered submarine basalts. *Canadian J. Earth Sci.*, v. 9, p. 172-184.
- Mysen, B., 1976. Partitioning of samarium and nickel between olivine, orthopyroxene, and liquid; preliminary data at 20 kbar and 1025°C, *Earth Planet. Sci. Lett.*, v. 31, p. 1-7.
- Nakamura, N., 1974. Determination of REE, Ba, Fe, Mg, Na and K in carbonaceous and ordinary chondrites, *Geochim. Cosmochim. Acta*, v. 38, p. 757-775.
- O'Neil, J. R. and Taylor, H. P., 1967. The oxygen isotope thermometry of mafic igneous rocks, *J. Geology*, v. 79, p. 715-729.
- O'Nions, R. K. and Pankhurst, R. J. (1976): Sr isotope and rare earth element geochemistry of DSDP Leg 37 basalts, *Earth Planet. Sci. Lett.*, v. 31, p. 255-261.
- Pineau, F., Javoy, M., Hawkins, J. W., and Craig, H., 1976. Oxygen isotope variations in marginal basin and ocean ridge basalts. *Earth Planet. Sci. Lett.*, v. 28, p. 299-307.
- Schock, H. H., 1973. Instrumentelle Neutronenaktivierungsanalyse von Gesteinen am Beispiel von 7 Standardgesteinen des US Geological Survey, *Fresenius'Z. Anal. Chem.*, v. 263, p. 100-107.

- _____, 1977a. Comparison of a coaxial Ge(Li)- and a planar Ge-detector in instrumental neutron activation analysis of geologic materials, *J. Radioanal. Chem.*, v. 36, p. 557-564.
- _____, 1977a. Trace element partitioning between phenocrysts of plagioclase, pyroxenes and magnetite and the host pyroclastic matrix, *J. Radioanal. Chem.*, v. 38, p. 327-340.
- Sun, C. O., Williams, R. J., and Sun, S. S., 1974. Distribution coefficients of Eu and Sr for plagioclase-liquid and clinopyroxene-liquid equilibria in oceanic ridge basalt: an experimental study, *Geochim. Cosmochim. Acta*, v. 38, p. 1415-1433.
- Suzouki, T. and Epstein, S., 1976. Hydrogen isotope fractionation between OH-bearing minerals and water, *Geochim. Cosmochim. Acta*, v. 40, p. 1229-1240.
- Taylor, H. P., Jr., 1968. The oxygen isotope geochemistry of igneous rocks, *Contrib. Mineral. Petrol.*, v. 19, p. 1-71.
- _____, 1974. Oxygen and hydrogen isotope evidence for large scale circulation and interaction between ground waters and igneous intrusions, with particular reference to the San Juan volcanic field, Colorado. In Hofmann, A. W., Giletti, B. J., Yoder, H. S., Jr., and Yund, R. A. (Eds.), *Geochemical transport and kinetics*: Carnegie Inst. Washington Publ. 634, p. 294-324.
- Weill, D. F., McKay, G. A., Kridelbaugh, S. J. and Grutzeck, M. 1974. Modeling the evolution of Sm and Eu abundances during lunar igneous differentiation, Proc. Fifth Lunar Sci. Cont., *Geochim. Cosmochim. Acta*, Suppl. 5, v. 2, p. 1337-1352.
- Wenner, D. B. and Taylor, H. P., Jr., 1973. Oxygen and hydrogen isotope studies of the serpentinization of ultramafic rocks in oceanic environments and continental ophiolite complexes, *Am. J. Science*, v. 273, p. 207-239.
- Whittaker, E. J. W., and Muntus, R., 1970. Ionic radii for use in geochemistry. *Geochim. Cosmochim. Acta*, v. 34, p. 945-956.